A THREE-DIMENSIONAL PASSAGE FLOW ANALYSIS METHOD AIMED AT TURBOMACHINERY ELEMENTS

터보기계 요소 유동해석을 지향한 3차원 통로유동 해석법

Byeong Rog SHIN [1]
신 병 록

Incompressible developing entry flows through square ducts with 90 degree bends are studied numerically by using an efficient implicit SMAC scheme with different boundary conditions. This study eventually aimed at passage flow analysis of turbomachinery elements with a strong curvature such as centrifugal impeller or draft tube. The generalized implicit scheme used in the present study has been developted to solve the three-dimensional Navier-Stokes equations by the author. Numerical results for some different numerical conditions are obtained and compared with each other.

1. Introduction

The purpose of this paper is to develop an efficient computer code for solving the passage flow of turbomachinery with very complicated flow fields, and understand complex flow phenomena in a strongly curved duct which is to be basic physical elements associated with centrifugal impellers, diffusers and draft tubes. As compared with simple cross-section of the ducts, such flows induce complex secondary flows within the duct on account of existence of the curvature along the streamwise. These flows can result in large redistributions of the streamwise velocity, a pressure loss and increased heat transfer at the duct wall. From the engineering point of view, it is a important task to understand those flows accurately. As an example, draft tube in hydraulic turbine has a role to reduce the velocity and increase the pressure of the water discharging. This could have an important effect on the efficiency of the turbine, so better understanding of the flow behavior in the tube is highly required. For these reasons, many studies to analyze those flows have been made by experiments[1-3] and computations[4-5].

Recently as technologies advance, the gravity of studying to develop numerical schemes to simulate accurately those flows is high because better performance, compact and highly efficent designs are required in modern flow devices. Among numerical methods, the most widely used ones for computing the incompressible flow are the MAC type schemes and the pseudo-compressibility methods. The MAC type schemes[6-8] are an epoch-making method in which the continuity condition is satisfied identically and the spurious error, that is checkerboard like osillation of pressure, is removed completely by introducing a staggered grid. On the other hand, the pseudo-compressibility method[9-10] based on the compressible flow scheme have been used only for the steady state flow because of its hyperbolic character. However, recently this method has been extended to the unsteady flow by Kwak et al.[11]. The author has already proposed some implicit SMAC schemes and applied to laminar and turbulent flow problems. In these schemes, a staggered grid in curvilinear coordinates is applyed, and the elliptic equation of pressure is solved by using the vectorized Tschebyscheff SLOR method. Therefore, the elliptic character of incompessible flow is satisfied well.

In this paper, as a primary stage of developing a computer code for analyzing turbomachinery flow, a numerical simulation of laminar flow phenomena in 90° bends is performed using one of the above implicit SMAC scheme[12]. In the present study, the geometry of the curved area is the same as that of Humphrey et al.[1]. Detailed observations of the secondary flows obtained

1. Dept. of Mechanical Design Eng., Chungnam Nat'l University (Yusung, Daejeon 305-764, Tel: 042-821-6645)

under the several different entrance and exit boundary conditions are made. Also, comparisions of predicted present results with available experimental data are provided.

2. Governing Equations

The governing equations of the present scheme are the 3-D incompressible Navier-Stokes equations of the volume fluxes JU_ℓ in curvilinear coordinates written as[12]

$$\frac{\partial}{\partial t}(JU_\ell) + L(JU_\ell, p) = 0 \qquad (\ell = 1,2,3) \tag{1}$$

$$\frac{\partial}{\partial \xi_i}(JU_i) = 0 \tag{2}$$

where

$$L(JU_\ell, p) \equiv \frac{\partial}{\partial \xi_i}(JU_iU_\ell) - JU_i\boldsymbol{u}\cdot\frac{\partial}{\partial \xi_i}\nabla\xi_\ell + \tilde{g}_{\ell i}\frac{\partial p}{\partial \xi_i} + \nu\epsilon_{\ell ij}\frac{\partial}{\partial \xi_i}h_{jk}Z_k \quad (\ell = 1,2,3) \tag{3}$$

and $\tilde{g}_{ij}=Jg_{ij}$. $\epsilon_{\ell ij}$ is the permutation tensor. The Jacobian J and the metrics g_{ij} and h_{ij} of the transformation from cartesian coordinates $\boldsymbol{x}[=(x,y,z)]$ to general curvilinear coordinates $\boldsymbol{\xi}[=(\xi,\eta,\zeta)]$ are $J = \partial(x,y,z)/\partial(\xi,\eta,\zeta)$, $g_{ij}=\nabla\xi_i\cdot\nabla\xi_j$ and $h_{ij}=\partial\boldsymbol{x}/\partial\xi_i\cdot\partial\boldsymbol{x}/\partial\xi_j$, respectively. And the relations between the physical velocity $\boldsymbol{u}$ in $\boldsymbol{x}$ space and the contravariant velocity $\boldsymbol{U}$ in $\boldsymbol{\xi}$ space are $U_i=(\partial\xi_i/\partial x_j)u_j$ and $u_i=(\partial x_i/\partial\xi_j)U_j$ using the summation convention. Similarly the contravariant vorticity $\boldsymbol{Z}$ and physical vorticity $\boldsymbol{\zeta}$ are defined as $Z_i=(\partial\xi_i/\partial x_j)\zeta_j$ and $\zeta_i=\nabla\times\boldsymbol{u}=(\partial x_i/\partial\xi_j)Z_j$.

By applying the forward Euler method to Eq.(1), but the implicit Euler method to the pressure term, the explicit SMAC scheme for the governing equations (1) and (2) can be derived as follows:

$$JU_\ell^* = JU_\ell^n - \Delta t L(JU_\ell, p)^n \quad (\ell = 1,2,3) \tag{4}$$

$$\frac{\partial}{\partial \xi_\ell}(\tilde{g}_{\ell i}\frac{\partial\phi}{\partial\xi_i}) = \frac{1}{\Delta t}\frac{\partial}{\partial\xi_\ell}(JU_\ell^*) \tag{5}$$

$$JU_\ell^{n+1} = JU_\ell^* - \Delta t\tilde{g}_{\ell i}\frac{\partial\phi}{\partial\xi_i} \quad (\ell = 1,2,3) \tag{6}$$

$$p^{n+1} = p^n + \phi \tag{7}$$

where

$$JZ_i = \epsilon_{\ell ij}\frac{\partial}{\partial\xi_i}(\tilde{h}_{jk}JU_k) \quad (j = 1,2,3), \tag{8}$$

$\tilde{h}_{ij}=h_{ij}/J$, the asterisk * denotes the intermediate time level and ϕ is the pressure increment. In this explicit SMAC scheme, the volume fluxes JU_ℓ^{n+1} obtained from Eq.(6) are made to satisfy the continuity condition (2) identically when Eq.(5) are satisfied sufficiently.

3. Numerical Algorithms

Equation (4) is extend to an implicit scheme by applying the Euler forward-difference scheme and the trapezoidal rule. Further, linearizing nonlinear terms at the intermadiate step by using the known values of time step n and applying the delta-form approximate-factorization scheme[13], Eq.(4) becoms as[12]

$$\{1 + \Delta t\theta(\frac{\partial}{\partial\xi}U^n - \nu\frac{\partial}{\partial\xi}\tilde{h}_{22}\tilde{h}_{33}\frac{\partial}{\partial\xi})\}\{1 + \Delta t\theta(\frac{\partial}{\partial\eta}V^n - \nu\frac{\partial}{\partial\eta}\tilde{h}_{33}\frac{\partial}{\partial\eta}\tilde{h}_{11})\}\cdot$$
$$\{1 + \Delta t\theta(\frac{\partial}{\partial\zeta}W^n - \nu\frac{\partial}{\partial\zeta}\tilde{h}_{22}\frac{\partial}{\partial\zeta}\tilde{h}_{11})\}\Delta JU^* = RHS_1^n \tag{9}$$

$$\{1+\Delta t\theta(\frac{\partial}{\partial\xi}U^n-\nu\frac{\partial}{\partial\xi}\tilde{h}_{33}\frac{\partial}{\partial\xi}\tilde{h}_{22})\}\{1+\Delta t\theta(\frac{\partial}{\partial\eta}V^n-\nu\frac{\partial}{\partial\eta}\tilde{h}_{33}\tilde{h}_{11}\frac{\partial}{\partial\eta})\}\cdot$$
$$\{1+\Delta t\theta(\frac{\partial}{\partial\zeta}W^n-\nu\frac{\partial}{\partial\zeta}\tilde{h}_{11}\frac{\partial}{\partial\zeta}\tilde{h}_{22})\}\Delta JV^*=RHS_2^n \tag{10}$$

$$\{1+\Delta t\theta(\frac{\partial}{\partial\xi}U^n-\nu\frac{\partial}{\partial\xi}\tilde{h}_{22}\frac{\partial}{\partial\xi}\tilde{h}_{33})\}\{1+\Delta t\theta(\frac{\partial}{\partial\eta}V^n-\nu\frac{\partial}{\partial\eta}\tilde{h}_{11}\frac{\partial}{\partial\eta}\tilde{h}_{33})\}\cdot$$
$$\{1+\Delta t\theta(\frac{\partial}{\partial\zeta}W^n-\nu\frac{\partial}{\partial\zeta}\tilde{h}_{11}\tilde{h}_{22}\frac{\partial}{\partial\zeta})\}\Delta JW^*=RHS_3^n \tag{11}$$

where

$$RHS_\ell^n=-\Delta tL(JU_\ell,p)^n \quad (\ell=1,2,3), \quad JU_\ell^*\equiv JU_\ell^n+\Delta JU_\ell^* \quad (\ell=1,2,3)$$

and $0\leq\theta\leq1$. This delta formed implicit SMAC scheme is satisfies a diagonally dominant condition with the first order upstream difference and is the TVD stable for $\theta=1$. This implicit SMAC scheme is suitable for vector or vector parallel machine as compared with the HSMAC scheme and the SIMPLE scheme developed toward scalar machine[14].

Equations (9)-(11) can be solved by dividing into them three steps, and each step is the problem solving the simultaneous equations with tri-diagonal matrix by the Gaussian elimination. The second-order central-difference scheme is basically used for the space derivatives. However, the Chakravarthy-Osher TVD upwind difference scheme[15] is applied to the convection term in the RHS_ℓ.

4. Numerical Results

Three cases of an incompressible developing entry flow through a square duct with 90 degree bend are computed by using the present implicit SMAC scheme. The cross section of the bend is square throughout the bend[1]. The Reynolds number based on the inlet mean velocity (U_0) and the entrance width (H) is 790. The mean radius of the bend is 2.3. Figure 1 illustrates the computational geometry, nomenclature and coordinate system.

For the boundary conditions, no-slip condition and von Neumann condition for the pressure were implemented on the solid wall boundary. And, the uniform flow and constant pressure were imposed on the inlet and outlet boundary, respectively. The entrance and exit boundary locations and used grid points of the three cases of flow field are listed in Table 1.

In Fig.1 and Table 1, X_U and X_D are represent the length of inlet and outlet boundaries from the bend, respectively. For all cases, the streamwise spacing at the bend area is 2.5°. In the present computation of the Case I and II, both results are also the same for the different exit

Table 1 Entrance and exit boundary locations and grid points

	Boundary location		Grid points
	X_U (H)	X_D (H)	($X\times Y\times Z$)
Case I	7.5	5	101×41×41
Case II	7.5	7.5	107×41×41
Case III	9	5	107×41×41

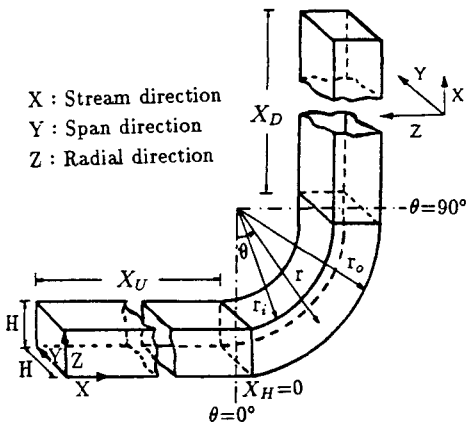

Fig. 1 Computational geometry

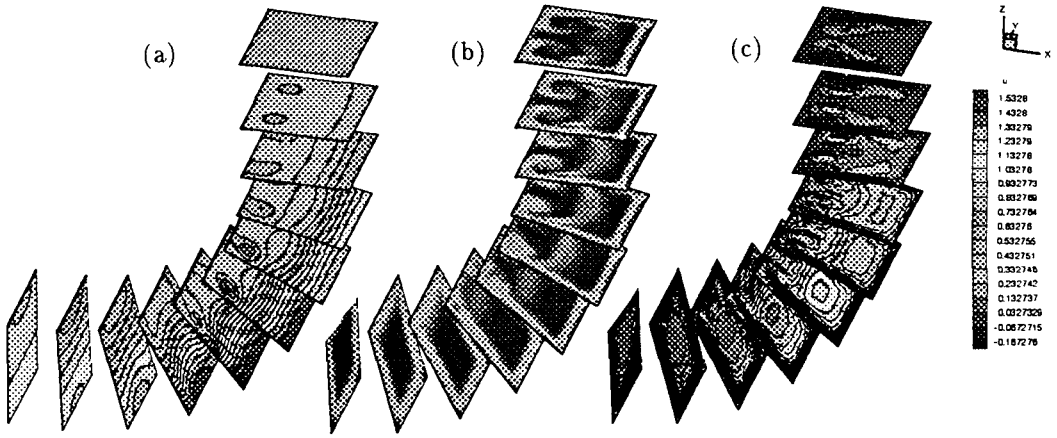

Fig. 2 Numerical results of (a) pressure contours, (b)vorticity magnitude contours and (c) streamwise velocity magnitude contours (Case III)

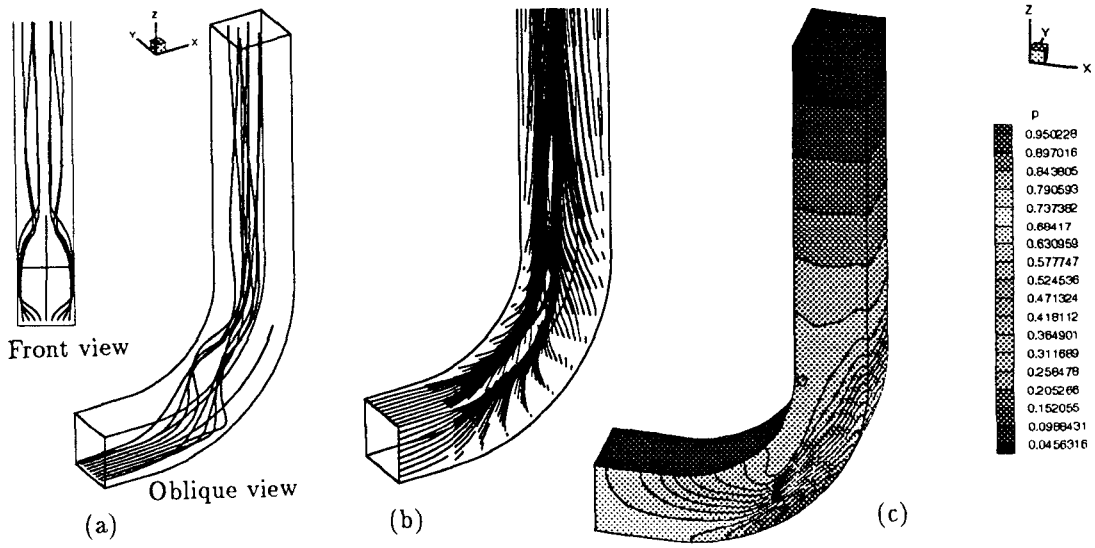

Fig. 3 Numerical results of (a) streamlines, (b)oil flow patterns and (c) surface pressure distributions (Case III)

boundary and same Dirichlet condition for the pressure. However, the results obtained from the Case III were closer to experiments[2] than that of the Case I and II. The discrepancy of the results among the three cases is small, but it seems to be due to the effect of the inlet conditions which is related to thickness of the boundary layer at entrance of the bend. Such effect was also observed by Govindan et al.[16].

Figure 2 shows the numerical results of pressure contours, voticity magnitude contours and streamwise velocity magnitude contours at several streamwise cross sections. In the bended area, relatively high pressure are distributed near the outside wall. It shows that the secondary vortices are formed at both sides from the center of the duct, and this vortex pair is seen to become stronger and move toward the inside wall (Fig.2(b)). On the other hand, the center of the high velocity flow moves to outer wall with the angle of θ (Fig.2(c)), which is due to the secondary flow formed by the curvature. Near the end of the bend, this center is shifted to both side corners of the outer wall, and the second high velocity region is formed near the inner wall. Figure 3(a) shows streamlines viewing from the two different view points. The vortex

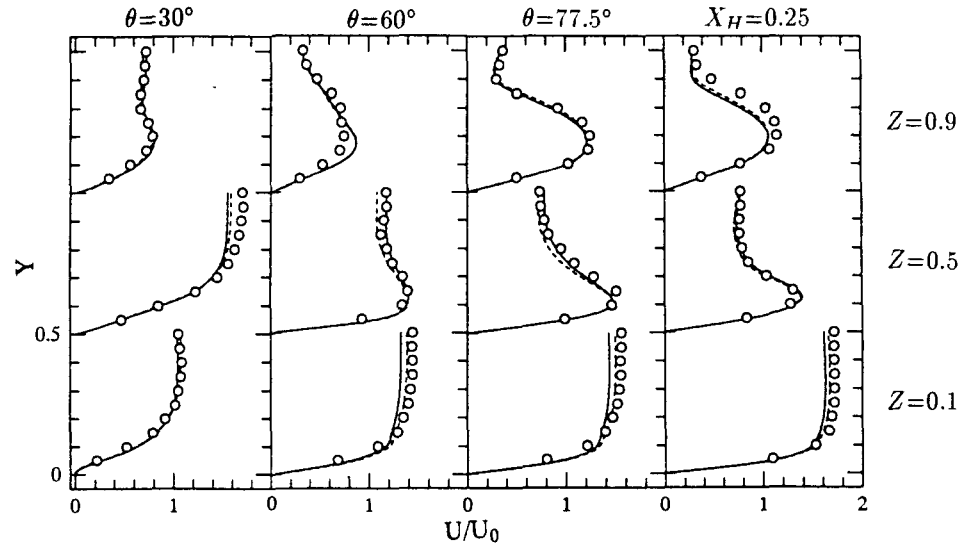

Fig. 4 Streamwise velocity profiles: —, Case I; ---, Case III; ○, Experiments[2]

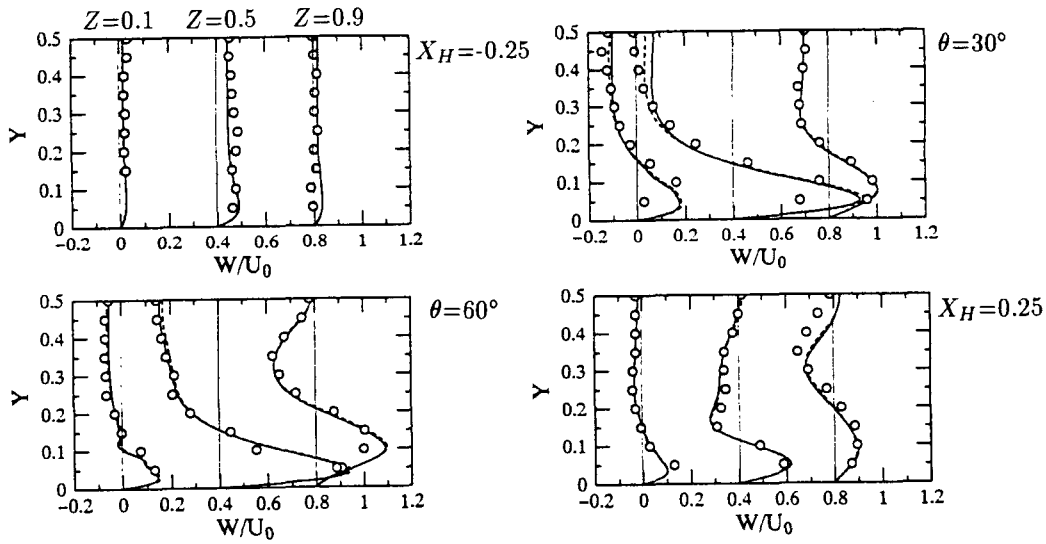

Fig. 5 Secondary velocity profiles: —, Case I; ---, Case III; ○, Experiments[2]

pair originated at begining of the bend is observed. Also, the separation region can be seen in Fig.3(b) of the oil flow pattern on the inside wall. Figure 3(c) shows the surface pressure distribution. As mentioned in Fig.2, the pressure on the outer wall is much higher than that of the inner wall due to the centrifugal forces. At downstream from the bend, the pressure is recovered to the uniform value across the cross-section.

Figure 4 shows a comparison of streamwise velocity profiles along the Y lines with experimental data[2]. As mentioned above, the Case III predicts better. The agreement between predictions and measurements is good at most locations. In the inner wall region, the velocity near both side walls is large with the θ. And Fig.5 compares the predicted secondary velocity w with experiments[2]. The present computations well capture the peak value of w and all the qualitative features of the flow. Figures6(a)-(c) show streamwise velocity vectors on the left hand side wall (Y=0.99) and outer wall (Z=0.01), on the inner wall (Z=0.99) and the right

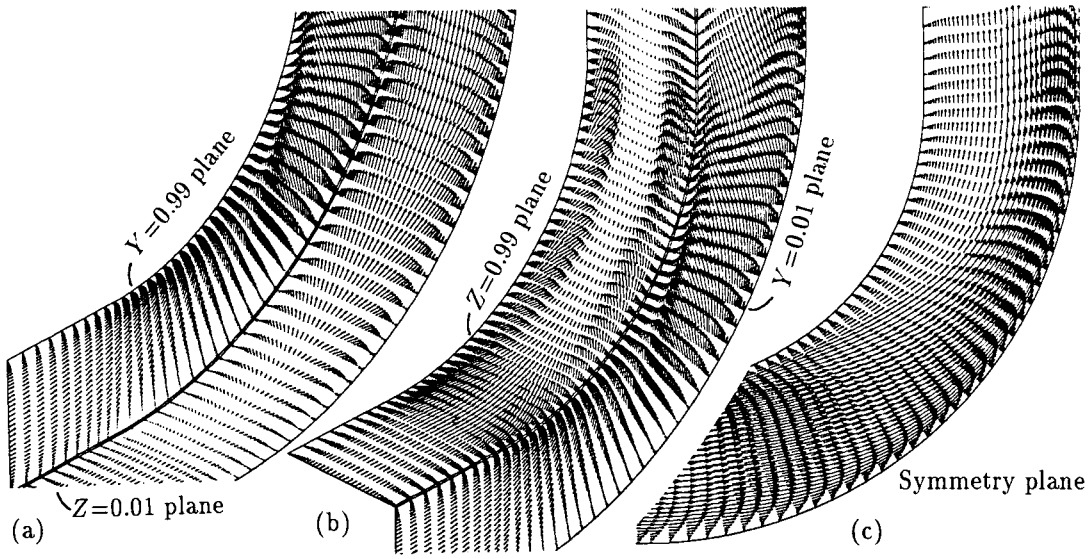

Fig. 6 Streamwise velocity vectors (Case III)

hand side wall (Y=0.01), and on the symmetry plane (Y=0.5). Redistributions of the velocity along the streamwise direction and the recirculation zone which is formed at both side corners of the out side wall near 5°~40° are seen in this figure. In this computation, the second maximum velocity occurs near 50°.

5. Conclusions

An incompressible developing entry flow through a square duct with a 90 degree bend is studied numerically by using an efficient implicit SMAC scheme which developed previously for solving the three dimensional Navier-Stokes equations in general curvilinear coordinates. In the present computation, three dimensional complex flow phenomena including strong secondary motion in the curved duct are simulated well. And a good agreement with experimental data is obtained indicating the high reliability of the present scheme for computing the 90 degree bended duct or similar duct with a strong curvature.

References

[1] Humphrey, J.A.C., et al., (1977) *J. Fluid. Mech.*, Vol.83, Part 3, pp.509-527.
[2] Taylor, A.M.K.P., et al., (1982) *Trans. ASME J. Fluid Eng.*, Vol.104, No.9, pp.350-359.
[3] Akiyama, M., et al., (1984) *Trans JSME Ser. B*, Vol.50, No.449, pp.286-292.
[4] Sotirpoulos, F., Kim, W.J. and Patel, V.C., (1994) *Computers Fluids*, Vol.23, No.4, p.627.
[5] Cabuk, H., Sung, C.H. and Modi, V., (1992) *AIAA J.*, Vol.30, No.8, pp.2024-2031.
[6] Hallow, F.H. and Welch, J.E., (1965) *Phys. Fluids*, Vol.8, No.12, pp.2182-2189.
[7] Amsden, A.A. and Harlow, F.H., (1970) *J. Comput. Phys.*, Vol.6, No.2, pp.322-325.
[8] Kim, J. and Moin, P., (1985) *J. Comput. Phys.*, Vol.59, No.2, pp.308-323.
[9] Chorin, A.J., (1967) *J. Comput. Phys.*, Vol.2, No.1, pp.12-26.
[10] Chang, J.L.C., et al., (1988) *Int. J. Numer. Methods Fluids*, Vol.8, No.10, pp.1241-1268.
[11] Rogers, S.E., Kwak, D. and Kiris, C., (1991) *AIAA J.*, Vol.29, No.4, pp.603-610.
[12] Ikohagi, T., Shin, B.R. and Daiguji, H., (1992) *Computers Fluids*, Vol.21, No.2, pp.163-175.
[13] Beam, R.M. and Warming, R.F., (1978) *AIAA J.*, Vol.16, No.4, pp.393-402.
[14] Shin, B.R., Ikohagi, T. and Daiguji, H., (1995) *CFD J.*, Vol.4, No.2, pp.191-208.
[15] Chakravarthy, S.R. and Osher, S., (1985) *AIAA Paper* No.85-0365.
[16] Govindan, T.R., Briley, W.R. and McDonald, H., (1991) *AIAA J.*, Vol.29, No.3 pp.361-370.